THE ASTROPHYSICAL JOURNAL, 403:385–395, 1993 January 20

THE DISTANT FUTURE OF SOLAR ACTIVITY: A CASE STUDY OF β HYDRI. I. STELLAR EVOLUTION, LITHIUM ABUNDANCE, AND PHOTOSPHERIC STRUCTURE[1]

D. DRAVINS,[2] L. LINDEGREN,[2] Å. NORDLUND,[3] AND D. A. VANDENBERG[4]

Received 1992 January 28; accepted 1992 July 23

ABSTRACT

The post–main-sequence evolution of stellar activity and of nonthermal processes in solar-type atmospheres is studied through a detailed comparison of the current Sun (G2 V) with the very old solar-type star β Hyi (G2 IV). Magnetically related activity decreases with age, and in very old stars one might possibly find the "absolute minimum" of stellar activity. In the solar galactic neighborhood, the closest single solar-type star, with an old age well-determined from evolutionary tracks, is β Hyi (HR 98, HD 2151; G2 IV). Its successive atmospheric layers are analyzed in a series of papers, where this Paper I treats general stellar properties and the deeper atmosphere. Following a critical review of data from various sources, the age of β Hyi is determined from evolutionary models to 9.5 ± 0.8 Gyr, twice that of the Sun. Its proximity to the main sequence in the Hertzsprung-Russell diagram tells it originated from near the solar position of G2 V. Being the closest subgiant, β Hyi is a bright target and has been observed under very high spectral resolution. A relatively high lithium abundance may be a signature of the early subgiant stage, when lithium that once diffused to beneath the main-sequence convection zone is dredged up to the surface as the convection zone deepens. Numerical simulations of the three-dimensional photospheric hydrodynamics show typical granules to be significantly larger (a factor of $\simeq 5$) than solar ones. The photospheric pressure is smaller, thus limiting the flux density to which photospheric magnetic fields can be compressed. The lower surface gravity and density leads to greater granular velocities (a factor of $\simeq 1.5$–2), since the same surface energy flux as in the Sun must be carried by lower density gas. Synthetic Fe I photospheric line profiles computed from these ab initio hydrodynamic models are compared to those observed at very high resolution ($\lambda/\Delta\lambda \simeq 200{,}000$). The line cores indicate a stellar rotation $v \sin i = 2 \pm 1$ km s^{-1}, while the line wings suggest the presence of transonic or supersonic motions in the more vigorous granulation on this subgiant.

Subject headings: stars: abundances — stars: atmospheres — stars: evolution — stars: individual (β Hydri) — Sun: activity

1. THE EVOLUTION OF SOLAR ACTIVITY

The study of solar activity forms the basis for understanding stellar activity and, conversely, studies of activity in solar-type stars aid in understanding solar phenomena. In particular, correlations of secular activity changes with variations in the general properties of evolving stars may give clues to an understanding of the basic mechanisms involved. Besides their astrophysical interest, such changes of solar magnetic activity may have a profound influence on the Earth's climate, but the fundamental mechanisms behind them are still largely unknown. A major limitation is the lack of *detailed* comparison data for other solar-type stars. Although various activity indicators have been observed for many stars, it has not been possible to choose samples of stars with well-understood evolutionary histories and other properties, permitting only rough comparisons with the Sun. The difficulty of studying detailed physical processes in distant stars makes it awkward to identify the precise parameters behind the secular evolution of solar activity, even though solar-type stars show the strongest age evolution of, e.g., coronal activity among all spectral types. A tantalizing possibility is offered by the study of stars almost identical to the Sun, whose parameters can then be interpreted in terms of (perturbed) solar models. In particular, a careful selection of stars virtually identical to the Sun, except for age, permits the study of the probable past history and distant future of solar activity.

Young stars are normally identified through their membership in young and undispersed galactic open clusters, and they are usually characterized by much stronger chromospheric and coronal emission than in the present Sun. Such activity can readily be detected, and young stars have been studied by many authors. This activity in young stars is generally believed to be related to their magnetic fields, decreasing with stellar age. Thus, in very old stars one could hope to identify some signature of, e.g., the "basal" (nonmagnetic) chromosphere, which must exist due to heating through acoustic processes. However, *old* stars are much more difficult to study, both because of their generally much lower activity levels, and the difficulty of age determination. Although old stars can be found among the members of distant globular clusters, the apparent brightness of such stars is much too low to permit any detailed observational studies.

The nearest stars are important targets because they permit observations with the highest possible spectral resolution, and because the determination of their physical parameters is not plagued by distance uncertainties. The immediate galactic

[1] Based in part on observations collected at European Southern Observatory, La Silla, Chile.

[2] Lund Observatory, Box 43, S-22100 Lund, Sweden.
[3] Copenhagen University Observatory, Øster Voldgade 3, DK-1350 Copenhagen, Denmark.
[4] Dept. of Physics and Astronomy, University of Victoria, P.O. Box 3055, Victoria, B.C., Canada V8W 3P6.

neighborhood includes two stars that are very similar to the Sun (G2 V), except for age. One of these is α Cen A (HR 5459; G2 V), a slightly evolved star that is a member of a multiple star system, and apparently somewhat older than the Sun. Its chromosphere and corona has been studied by various authors, but detailed comparisons to the Sun may be somewhat hampered by the ignorance of whether evolution in stellar magnetic activity might be different for a single star or a binary system. Also, although α Cen A is somewhat evolved from the zero-age main sequence, it is "only" in the upper part of the main-sequence band, and existing small uncertainties in, e.g., its mass, may lead to significant uncertainties in its age. The other star is β Hyi (HR 98, HD 2151; G2 IV), a single star about twice as old as the Sun.

β Hyi is the closest subgiant and one of the oldest stars in the solar galactic neighborhood. It is a nearby star with a well-determined trigonometric parallax, and with good photometry and spectroscopy available. Its position in the Hertzsprung-Russell diagram places it among those rather few evolved field stars whose ages can be determined without ambiguity from theoretical evolutionary tracks. It is close enough to the main sequence to tell that it originated there from around G2 V, near the solar position. At the same time, it is almost as old as a solar-mass star can be, and still be possible to accurately date from stellar evolutionary theory. (A much more evolved single field star would be ambiguous because evolutionary tracks of more massive stars cross the H-R diagram somewhat further from the main sequence.)

By all appearances, β Hyi is a fully normal, single star. Thanks to its proximity it is a very bright target, allowing detailed observations. It may well represent the future Sun, and its study allows an exploration of the likely state of solar activity in the distant future, as well as a general illustration of the post–main-sequence evolution of nonthermal processes in solar-type atmospheres. Indeed, analyses of chromospheric activity indicators versus stellar age suggest that the age-activity relation of solar-type stars is *deterministic* (i.e., not merely statistical), underscoring the value of studying individual well-understood stars (Soderblom, Duncan, & Johnson 1991). The aim of this work is to take this star as a likely representative of the future Sun, and then to pursue a comprehensive study of different phenomena in this star, along with a discussion of its general evolutionary status, to illustrate a probable scenario for the distant future of solar activity.

The properties of β Hyi will be contrasted to those of the Sun and discussed in sequence from the stellar interior, and out through the atmosphere in a series of three papers. The present Paper I is devoted to basic stellar data (§ 2), analysis of the stellar evolutionary status, properties of the convection zone (in particular as reflected in the lithium abundance; §§ 3–4), the structure of the photospheric granulation as analyzed through numerical simulations, and the predicted appearance of the photospheric line spectrum, also observed under very high spectral resolution (§ 5). Section 6 concludes Paper I by summarizing the main changes of the photosphere and deeper layers from the present Sun to β Hyi.

Paper II (Dravins et al. 1993a) discusses chromospheric signatures and their time variability, while Paper III (Dravins et al. 1993b) is devoted to the hottest layers of the outermost atmosphere: the transition region and corona.

2. β HYDRI: THE STAR

The apparent brightness of β Hyi ($m_v = 2.80$ mag) has permitted detailed spectroscopic and other studies of its properties. In this section, we review the present understanding of its general properties and evolutionary status in relation to the present Sun.

2.1. *Fundamental Stellar Properties*

2.1.1. *Spectral Type*

The spectral type is G2 IV (Hoffleit & Jaschek 1982; Evans, Menzies, & Stoy 1957), almost identical to that of the Sun (G2 V). Occasionally it has been quoted also as G1 IV.

2.1.2. *Temperature*

A well-determined temperature equals the solar one within 100 K. Hearnshaw (1972) used photoelectric scans, Hα wing profiles, and $R-I$ colors to determine $T_{\rm eff} = 5730$ K. Gehren (1981) deduced 5880 ± 100 K from Hα and Hβ profiles, similar to the value by Proust & Foy (1988; 5860 K). From photometric indices, Gratton & Ortolani (1986) find 5750 K. Here, we adopt 5800 ± 100 K as a likely value, equal to the commonly accepted value for the Sun of $T_{\rm eff} = 5780 \pm 30$ K.

2.1.3. *Surface Gravity*

This was determined spectroscopically by Hearnshaw (1972) against a grid of model atmospheres to $\log g = 1.8 \pm 0.2$ (m s^{-2}). Other determinations in this range exist in the literature: e.g., 1.75 (Gratton & Ortolani 1986); 2.0 (Proust & Foy 1988). From the parallax and calibrated photometry Gehren (1981) obtained 2.15. The solar value is 2.44 (=4.44 cm s^{-2}). The numerical simulations of photospheric granulation (§ 5) use the value 1.84. Part of a grid of models, that value was chosen to be a factor of 4 less than the solar one, while being representative for β Hyi. For our age determination, the absolute visual magnitude will be used.

2.1.4. *Metallicity*

The chemical evolution of the Galaxy can be traced through low metal abundances in those stars that formed while the Galaxy was still young, and β Hyi follows this pattern. The metallic absorption lines are noticeably weaker than solar, and a number of authors have analyzed the abundances of various elements. As expected for an old star, β Hyi is slightly metal poor, with log [Fe/H] determinations relative to the Sun in the range 0 to −0.3 (Rodgers & Bell 1963; Hearnshaw 1972; Gehren 1981; Rebolo et al. 1986; Proust & Foy 1988). From these we adopt the value −0.2, which will be used in some of the discussions below. For line identifications in the near-ultraviolet spectrum, see Beckman, Crivellari, & Selvelli (1982).

2.1.5. *Rotation*

β Hyi is a slow rotator, and the rotational broadening is only a minor component of its spectral line widths. In fitting line profiles from hydrodynamic model atmospheres, Dravins & Nordlund (1990b) obtained $v \sin i = 2 \pm 1$ km s^{-1}. The rotational velocity at the solar equator is 1.8 km s^{-1}. Since the radius of β Hyi is about $1\frac{1}{2}$ times solar, a given velocity implies a correspondingly longer rotational period. Assuming the rotational axis in the plane of the sky, 2 km s^{-1} implies a period of approximately 45 days.

2.1.6. *Parallax and Luminosity*

Thanks to the proximity of β Hyi, its trigonometric parallax and distance can be accurately determined. Its parallax has been measured from the Cape Observatory and from the Yale-Columbia Southern Station. Evaluating these sources, the General Catalogue of Trigonometric Stellar Parallaxes lists the absolute parallax as 0".153 ± 0".007 (Jenkins 1952). This trans-

lates to a distance of 6.5 ± 0.3 pc, making β Hyi the closest subgiant.

Its apparent visual magnitude m_v equals 2.80, and its absolute magnitude then follows from the parallax: $M_v = 3.72(\pm 0.1)$, a full magnitude more luminous than the Sun ($M_v = 4.83$).

2.1.7. *Photometry and Luminosity*

The position of β Hyi relative to the zero-age main sequence (ZAMS) in the Hertzsprung-Russell diagram can be determined through *uvbyβ* photometry in the Strömgren system. Such studies by Crawford (1975) indicate the absolute magnitude of β Hyi to be $M_v = 3.77$, fully consistent with the value deduced from the parallax. The mean value of $M_v = 3.745$ means a factor 2.7 brighter than the Sun and, at equal effective temperature, corresponds to a stellar radius $R_* = 1.6\ R_\odot = 1.15 \times 10^9$ m.

2.1.8. *Single Star*

It is a single star, with no indications of duplicity. Such would have been readily seen from variations in its large proper motion (2".3 per year; Eggen 1958), or in its radial velocity which has been repeatedly measured since 1903 and has remained constant (Abt & Biggs 1972). Some authors have even used β Hyi as a standard velocity star.

2.1.9. *Nonvariability*

β Hyi is a nonvariable star. It has been searched for microvariability, but none has been seen (Stobie 1971).

For the record, a clarification of an ambiguous item in the literature may be pertinent. β Hyi has been listed in catalogs of stars of suspected variability (Kukarkin et al. 1951, 1982), and these entries have been quoted in other, even very recent, star catalogs. The reason for its inclusion there turns out to be that it had been earlier listed as a suspected variable by Zinner (1929). An examination shows that it was included in this earlier publication because John Herschel had made visual observations of β Hyi from South Africa in the years 1835–1838, and his "magnitude," translated to the photographic magnitude scale of the early 1900s, came out fainter than those more modern values! While this is certainly no reason to suspect secular changes in the stellar luminosity, it is an example how quoting and requoting of antiquated observations may pervade even current literature.

2.1.10. *Galactic Orbit*

The older disk population in the Galaxy is characterized by relatively eccentric galactic orbits, and β Hyi is no exception. A member of the ζ Her group of high-velocity stars, it moves with 41 km s^{-1} relative to the local standard of rest. Its galactic orbit of eccentricity 0.18 carries it some 270 pc above the galactic plane (Eggen 1971; Hearnshaw 1972).

2.1.11. *Ambiguous Identifications*

More than one author has had difficulties distinguishing the constellations Hydra and Hydrus, and there exist numerous papers where β Hyi is mistakingly labelled "β Hya." When no additional designations are given, the stars can often be identified knowing that β Hydrae (HR 4552) is a hot B9 IIIp giant, with a spectrum rather different from that of β Hydri.

3. AGE AND EVOLUTIONARY STATUS

β Hyi is one among only rather few single stars, whose position in the H-R diagram permits its age to be accurately determined from evolutionary theory. While it has evolved well off the main sequence, it is still close enough to avoid ambiguities in stellar evolutionary tracks (theoretical isochrones cross only for somewhat more massive stars, which possess convective cores during their main-sequence phase). A few nearby G subgiants have evolved to about a magnitude above ZAMS, and β Hyi is the nearest among these. Provided reasonably accurate parallaxes are available, these are the only field stars with well-defined ages that are sufficiently bright for detailed observations.

A number of authors have evaluated the evolutionary age of β Hyi. In earlier work, Hearnshaw (1972, 1973) applied theoretical isochrones by Iben and by Aizenman, Demarque, & Miller, to arrive at a mean value of 8 Gy, while Perrin et al. (1977) obtained 10 Gyr from comparisons with models by Hejlesen. Cayrel de Strobel (1981) compared models by Ciardullo & Demarque to find 9 Gyr.

3.1. *Evolutionary Models*

In the present work, a number of stellar evolutionary tracks was computed, in order to permit a precise age determination. The stellar structure code described by VandenBerg (1983) and VandenBerg & Bell (1985) was used although, for reasons discussed by VandenBerg & Laskarides (1987), boundary conditions were based on an empirical T-τ relation (Krishna Swamy 1966) in preference to available theoretical model atmospheres. As in the recent study of AI Phe by Andersen et al. (1988), the mixing-length parameter was set so that a 1.0 $\mathfrak{M}_\odot$ model for $Z = 0.0169$ (the adopted solar metallicity) had an effective temperature of 5780 K at the solar age, which was taken to be 4.7 Gyr. The resultant value of the mixing-length parameter α, the ratio of the mixing-length to the pressure scale height, was 1.50. Requiring this model to have the solar luminosity yielded $Y = 0.27$ for the mass-fraction abundance of helium (when the latest Los Alamos opacities are assumed). Since β Hyi is observed to have a lower metal abundance than the Sun, $Y = 0.26$ has been adopted in all calculations for this star.

Figure 1 shows the evolutionary tracks away from the zero-

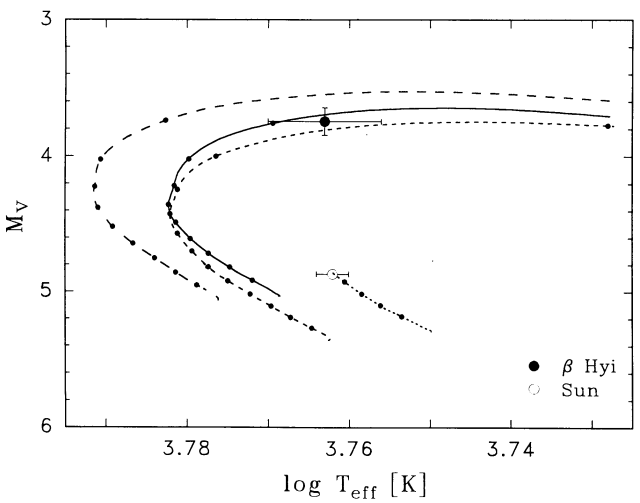

FIG. 1.—Stellar evolution and the age of β Hyi. Tracks away from the zero-age main sequence are shown for models spanning the parameter determinations of β Hyi. The solid curve is for stellar mass $\mathfrak{M} = 1.0\ \mathfrak{M}_\odot$ and metallicity [Fe/H] = −0.23, close to observed values. Dashed curves show lower mass stars, and superposed dots mark each Gyr away from ZAMS. Solar evolution from ZAMS to 4.7 Gyr is also shown (*dotted*), with the present Sun marked. The observed values indicate an age of ≃9.5 Gyr.

age main sequence for different stellar models spanning the range of parameter determinations of β Hyi, as well as for the Sun. The solid curve shows the evolution for a star with mass $\mathfrak{M} = 1.0\ \mathfrak{M}_\odot$ and metallicity [Fe/H] = −0.23, close to observed values. For this track, 81 models were computed for ages between ZAMS and 9.6 Gyr. Dashed curves show lower mass stars with the lower metallicity [Fe/H] = −0.45. The long-dashed one is for $\mathfrak{M} = 0.95\ \mathfrak{M}_\odot$, computed until 9.8 Gyr, the short-dashed one for $\mathfrak{M} = 0.90\ \mathfrak{M}_\odot$ until 12.0 Gyr. Using the best estimate for the luminosity from the parallax and photometry data discussed above: $M_v = 3.745$ mag ± 0.1, and $T_{\rm eff} = 5800 \pm 100$ K, we find (interpolating between the tracks) $\mathfrak{M} = 0.99\ \mathfrak{M}_\odot$, and age 9.5 Gyr if [Fe/H] = −0.23. As an extreme case for the metallicity [Fe/H] = −0.45, we would get $\mathfrak{M} = 0.92\ \mathfrak{M}_\odot$, and 10.4 Gyr. This age fits well with current estimates of the age of the Galactic disk (9–10 Gyr). The main observational uncertainty is due to the parallax error: about ± 0.8 Gyr, while errors in $T_{\rm eff}$ play almost no role since β Hyi is rapidly evolving nearly horizontally in the H-R diagram.

A number of stellar parameters may further influence the precise age determination, e.g., the ratio [O/Fe] (which, however, is close to solar; Gratton & Ortolani 1986). While a more detailed discussion of the exact age of β Hyi is beyond the scope of this paper, the general understanding of its evolutionary status should make it a very interesting object (in addition to the Sun) for testing stellar evolutionary models.

3.2. *Lithium Abundance*

Lithium is a fragile element and is destroyed at the temperatures and densities prevalent in stellar interiors. In the Sun, ^{7}Li burns at temperatures only slightly higher than those at the bottom of the surface convection zone. The surface abundance of ^{7}Li thus indicates to what extent the surface material has been mixed with the stellar interior, making lithium an important tool for probing stellar evolutionary history. Since lithium is not synthesized inside stars, and mechanisms for producing it on the surfaces of ordinary stars do not appear significant, it must become increasingly depleted with time. A number of authors have compared lithium abundances with other parameters and arrived at an empirical correlation with stellar age: younger stars have the most lithium. Such relations have been widely used to estimate stellar ages from observed abundances. For a general review, see Michaud & Charbonneau (1991).

While the abundances of heavier metals in β Hyi are characteristically low for an old star, its Li I resonance line at 670.7 nm is very much stronger than the solar one (Fig. 2, and, e.g., Feast 1966; Andersen, Gustafsson, & Lambert 1984; Maurice, Spite, & Spite 1984; Rebolo et al. 1986). Indeed, this is the most striking (known) difference between the entire photospheric spectra of β Hyi and the Sun. At the time of the original discovery by Feast, lithium in G stars was generally supposed to be significant only in young clusters.

We have repeated the observations of the lithium line region in β Hyi, trying to reach as high spectral resolution as possible. In Figure 2, this region is compared to the spectrum of the Sun seen as a star. Following some experiments with a single-pass scanner, β Hyi was observed with the ESO coudé echelle spectrometer in its common single-pass mode, using a Reticon multielement detector. The commonly used resolution there is $\lambda/\Delta\lambda = 100{,}000$, but we narrowed down the spectrometer entrance slit for a *nominal* resolution figure of $\lambda/\Delta\lambda \simeq 150{,}000$, although this value is not quite achieved, due to limitations in the imaging optics and the finite detector element sizes. The superposed integrated sunlight spectrum is that of the Sacramento Peak atlas (Beckers, Bridges, & Gilliam 1976), spectrally degraded to approximately correspond to the stellar spectrum, by convoluting it with an instrumental profile of similar resolution. The solar Li I doublet is barely discernible, while the Li feature is very prominent in β Hyi.

In the absence of other information, the lithium abundance of β Hyi could thus be taken as an indication of stellar youth and therefore merits additional comments. The deduced abundance of lithium depends on the effective temperature adopted for the model atmosphere, but very little on either the surface gravity or the assumed "microturbulence" parameter. This is because the observed lines are from neutral lithium (which is mostly ionized in the atmosphere), because it is a light element, and because the relevant Li lines are weak. The equivalent

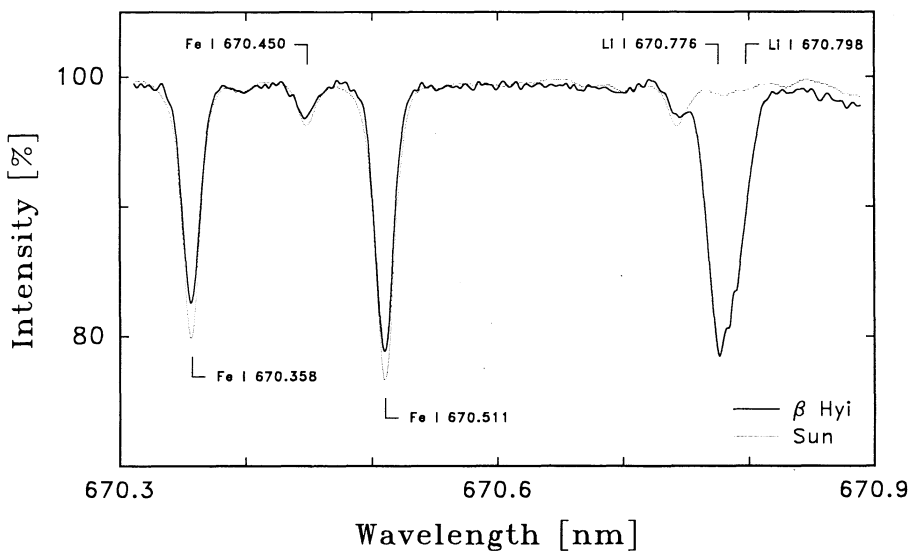

FIG. 2.—The Li I resonance line region in β Hyi (together with adjacent Fe I lines), compared to the spectrum of the Sun seen as a star. The solar Li I doublet is barely discernible, but prominent in β Hyi. This lithium enhancement on the stellar surface is suggested to be a result of the dredge-up of previously diffused lithium from the bottom of the convection zone, as this deepened during the early subgiant stages.

width of the Li I 670.7 nm feature in β Hyi is some 30 times the solar value, and a similar abundance ratio follows. Different authors have evaluated this abundance with a typical result [Li/H] $\simeq$ 1.4 (Feast 1970; Hearnshaw 1972; Andersen et al. 1984; Rebolo et al. 1986; Pallavicini, Cerruti-Sola, & Duncan 1987). On a scale where log N[H] = 12.00, the abundance by number in β Hyi is log N[Li] $\simeq$ 2.4. Some authors have also attempted to measure the isotope ratio ^{6}Li/^{7}Li, and recent analyses give an upper limit around the terrestrial and meteoritic ratio of 0.08 (Maurice et al. 1984; Rebolo et al. 1986; Pallavicini et al. 1987). If there had been a significantly greater fraction of ^{6}Li, it would have suggested Li production through spallation reactions on stellar surfaces. Beta Hyi thus shows a relative surface abundance of lithium an order of magnitude higher than that in the Sun. How can this be reconciled with the stellar age determination?

Recently, detailed analyses of lithium in various stars have demonstrated that the previous simple picture of an age-abundance relationship is not generally valid. Duncan (1981) made an extensive analysis of [Li] and chromospheric Ca II K emission in more than 100 F and G dwarfs and subgiants. He concluded that while these quantities statistically decrease in older stars, the correlation between them is not good. Duncan identified one group of nine "anomalous" stars, whose Li abundances are consistent with youth, while their K line emission is very weak, as if they were old. The old ages of several stars in this group could be confirmed by their large space motions in the Galaxy, and relatively low metallicities (average [Fe/H] = -0.17, not unlike β Hyi). Duncan concluded that Li abundance is not a good age indicator for these stars.

This study of stars in the northern sky was extended to 27 southern F8–G5 dwarfs and subgiants by Pallavicini et al. (1987). Their conclusions are similar to Duncan's. There exists a number of stars with low chromospheric emission, and high [Li] (but not the reverse). There are several old subgiants which are slowly rotating and chromospherically inactive, but have high [Li]. In a study of metal-deficient (and statistically old) dwarf stars, Rebolo, Molaro, & Beckman (1988) find a considerable spread in [Li] among stars of moderately low metallicity. Hobbs & Pilachowski (1988) find Li/H ratios exceeding the solar value by factors between 10 and 40 (again, similar to β Hyi) in very old solar-like stars in NGC 188, one of the oldest open clusters known. In their recent review of lithium abundance and chromospheric activity, Randich & Pallavicini (1991) again point out that the reasons for the high Li abundance in old solar-type stars like β Hyi are not understood.

Other recent discoveries have further complicated the picture. These include the discovery of significant lithium (comparable to that in β Hyi) in the oldest stars of the galactic halo. Another discovery was the lithium depletion (by two orders of magnitude) within a certain narrow temperature interval for F stars in clusters such as the Hyades. Such discoveries hint at the great sensitivity of [Li] to minor details in stellar structure or evolutionary history.

A number of authors have now discussed possible mechanisms behind the various abundance patterns. Perhaps the low metallicities in the halo stars have somehow influenced the convective patterns and helped to preserve the (cosmological?) lithium abundance to the present day? A most thorough and detailed model calculation for the evolution of surface lithium abundances from the pre–main-sequence phase to the giant branch is presented by Deliyannis, Demarque, & Kawaler (1990). This is a grid of theoretical evolutionary sequences for low-metallicity stars (corresponding to those in the galactic halo), reproducing the observations in halo stars as corresponding to the pregalactic lithium abundance. Although the fate of lithium depends on many parameters, these calculations are very instructive in illustrating processes likely to affect lithium also in solar-type stars. During the earlier main-sequence phase, the bottom of the convection zone is sufficiently hot to burn lithium, and depletion occurs. During the later main-sequence phases, diffusion may become increasingly efficient. A diffusion process (such as gravitational settling) in the radiatively stable layers beneath the convection zone (whose bottom is now at a lower temperature) can increase the lithium abundance in layers that are not hot enough for lithium burning. When the star then leaves the main sequence to evolve into a subgiant, the convection zone deepens, reaching these lithium-rich layers below. This lithium now replenishes and enriches the convection zone. Thus, during the early subgiant stages, the surface [Li] may quickly increase through this dredge-up from below. Eventually, the lithium abundance will again begin to decrease. From their extensive model calculations Deliyannis et al. (1990) thus conclude that simple age-[Li] relations are *not* reliable age indicators of field stars. They stress the importance of evaluating the stellar evolutionary status as prerequisites to understanding lithium abundances. Among data that are required to test the modeling of diffusion, they note the need for observations of the expected dredge-up enhancement for stars in their early subgiant phase.

Stellar evolutionary modeling should include also effects of stellar rotation, which generate three-dimensional mass motions, and which cannot be described by one-dimensonal models. Such modeling has been attempted for the Sun by Pinsonneault et al. (1989). Angular momentum is lost via a magnetic wind and is redistributed by rotationally induced instabilities. They conclude that rotationally induced mixing can reproduce the observed [Li] depletion in the Sun. This poses further problems for the use of [Li] as an age indicator, since the depletion will depend sensitively on each star's initial angular momentum. Observed rotation periods for subgiants may constrain such models. If main-sequence stars rotate as solid bodies, the rotation of subgiants should slow down markedly as their radius increases. If main-sequence stars instead possess differential rotation below their convection zone, they will bring up higher angular momentum material from below as they expand, leading to only a small decrease in rotation during the subgiant stage.

There is thus always the possibility that the rotational histories might differ from one solar-type star to the next, depending on the angular momentum distribution with which the star was born. High lithium abundances might remain in stars which were initially slowly rotating and never really experienced mixing. For a further discussion of the implications of differing initial angular momenta, see Simon (1992).

From our discussion we now conclude that the lithium abundance in β Hyi in no way appears to be unusual among old subgiants. The available detailed models (so far only for stars with somewhat different parameters) suggest a possible scenario for the lithium enhancement in β Hyi relative to the Sun: during the latter main-sequence lifetime an enhancement occurs through diffusion in the radiatively stable layers beneath the surface convection zone. This is followed by a dredge-up of lithium to the surface as the convection zone begins to reach deeper during the early subgiant stage. The

understanding of the surface lithium changes during stellar evolution requires a detailed understanding also of other stellar parameters. With its otherwise well-studied properties, β Hyi could indeed become a suitable object for testing detailed theories of lithium depletion, and of the evolution of rotation inside solar-type stars.

Beryllium survives to somewhat higher temperatures than lithium, and any depletion of its surface abundance provides evidence of mixing to greater depths. However, we have not made any such observations, and nor do there seem to exist any [Be] determinations for β Hyi in the literature.

4. THE CONVECTION ZONE

Somehow, the convection zone must supply the nonthermal energy that later finds its way up into the chromosphere and corona. The mechanism probably involves magnetic fields that are generated in some dynamo process and are being stretched and braided by the subsurface convective motions. This may be supplemented by acoustic waves generated by these gas motions. Thus the secular evolution of stellar subsurface structure is essential to the secular evolution of nonthermal phenomena in higher atmospheric layers.

4.1. *The Secular Evolution of the Convective Envelope*

Ruciński & VandenBerg (1986) computed the post–main-sequence evolution of convective envelopes of stars in the solar mass range and discussed the evolution of activity-related characteristics. They analyzed parameters of relevance to dynamo models, the amount of nonthermal energy available for dynamo action (in the form of gas motions in the deepest parts of the convection zone), and a number of length scales (such as pressure scale heights) throughout the convection zone. Their results show the maximum power available for activity to be essentially the same for solar metallicity, as for one-tenth its value.

Also, Gilliland (1985) studied how various stellar envelope parameters (convective turnover time scales, changes of the moment of inertia due to the redistribution of mass with radius, etc.) evolve along with the star off the main sequence. For a star such as β Hyi, the convection zone deepens, and the convective turnover time scale increases. At the same time, increases of the stellar moment of inertia result only in a moderate spin down.

A parameter of importance for stellar dynamo theories is the Rossby number $\mathfrak{R}_0 = P_{\rm rot}/\tau_{\rm conv}$, the ratio between the stellar rotation period and the convective turnover time inside the convection zone. The Rossby number is used in parameterized models of dynamo generation of magnetic fields, where it determines the extent to which rotation can induce both helicity and differential rotation required for dynamo activity in the convection zone. A smaller $\mathfrak{R}_0$ is expected to result in increased production of magnetic fields. Assuming solid-body stellar rotation, Gilliland (1985) finds that the Rossby number should decrease with stellar age, possibly leading to (renewed) dynamo activity in evolved stars.

Although a number of authors have correlated observed activity parameters with theoretical Rossby numbers, we feel that some of their conclusions could be premature since, for stars of comparable spectral type, their different Rossby numbers must mainly reflect different rotation periods, and a plot of, e.g., chromospheric activity against $\mathfrak{R}_0$ does then mainly show the (well-known) increase of activity with increasing stellar rotation (decreasing $P_{\rm rot}$ and decreasing $\mathfrak{R}_0$). Also, the basic physical concepts underlying the parameterization of dynamo theories are far from clear. For example, it is unknown how highly inhomogeneous magnetic structures interact with large-scale gas flows, and whether concepts such as "convective turnover time" correspond to any real physical process in stellar convection (quite apart from the question of computing its magnitude). Those few models of surface convection that have been made incorporating detailed hydrodynamic simulations rather indicate that the nature of convective motions is very different from a naive concept of overturning gas cells (e.g., Nordlund & Dravins 1990).

4.2. *p-Mode Oscillations*

Solar observations of global pressure-mode oscillations in velocity and brightness are used to constrain physical conditions at various depths beneath the photosphere. Computations of the p-mode spectra expected for a solar-composition 1 $\mathfrak{M}_\odot$ star, evolving from the ZAMS to the base of the giant branch (at age 11.5 Gyr), have been made by Guenther (1991). Several groups are attempting to observe these oscillations in solar-type stars. Beta Hyi was first observed by Frandsen (1987), who set an upper limit (at about 10 times the solar amplitude) for the temperature fluctuations that would have been visible in the intensity ratio between the spectral continuum and absorption line cores. Edmonds & Cram (1989, 1990, and private communication) made a more extensive search for velocity oscillations in β Hyi, using the 3.9 m Anglo-Australian Telescope, and might have a (marginal) suggestion of p-modes at periods around 7 minutes, and with a first-order frequency splitting close to the value expected from the general stellar properties. Thus present oscillation measurements tentatively confirm our previously determined parameters, but more precise data are required to yield new knowledge about the stellar interior.

5. THE PHOTOSPHERE

Although the detailed mechanisms of the energy supply to chromospheres and coronae are not at all completely understood, it is clear that a key role is played by the magnetic field. Irrespective of how that field has been generated, it must emerge through the photosphere and be modified by the granulation patterns there. The high electric conductivity of the photospheric material makes the magnetic fieldlines more or less "frozen-in," and they are affected by the gas flows. As the Sun evolves away from the main sequence, the photospheric conditions will gradually change, leading to a somewhat different atmospheric structure. We now examine these changes from the present Sun to β Hyi.

5.1. *Three-dimensional Models of Photospheric Granulation*

In recent years it has become possible to solve numerically the sets of hydrodynamic equations that realistically describe the three-dimensional time evolution of granular convection in the photospheres of solar-type stars (Nordlund 1982, 1985; Nordlund & Dravins 1990, and references therein). The equations of motion (describing the time evolution of the velocity field) and the energy equation (describing the time evolution of the temperature field) are used to step a three-dimensional numerical representation of the velocity and temperature fields forward in time. The use of realistic background physics (equation of state, absorption coefficients, etc.) taken from

standard stellar atmosphere code, a detailed treatment of the radiative transfer (nongray, three-dimensional), and the use of relevant boundary conditions (e.g., a penetrative lower boundary with constant heat input, and the absence of any walls or edges that could artificially constrain the flows) leads to a realistic simulation of granular convective motions.

Using the output from such simulations as sets of time- and space-dependent model atmospheres, synthetic absorption line profiles are obtained as spatial and temporal averages over the simulation sequence, permitting a direct comparison with observations. That such models do succeed in reproducing observed line profiles across the solar disk (including line asymmetries and wavelength shifts), indicates that photospheric structures (at least in nonmagnetic regions) are governed by only a few basic and well-understood physical laws, viz. radiative transfer and classical hydrodynamics. This does not mean that the resulting atmospheric structures could not be extremely complex, but since these laws of physics are mathematically known and computationally tractable, realistic simulations can be made already with current supercomputers.

Such models naturally contain a number of physical, mathematical, and numerical approximations. However, they contain no arbitrary *physical* parameters: the results depend in principle only on the effective temperature, surface gravity, and the chemical abundance. (These determine the heat flux into the simulation volume, the gravity forces stratifying the atmosphere, and the opacity of the gases, respectively.) Such ab initio models can be applied to stars with different temperatures, gravities, and metallicities.

5.2. *The Surface of β Hydri*

These computer codes, initially developed for solar conditions, were suitably modified, and such a numerical simulation was made also for a model with parameters corresponding to β Hyi. This model has the β Hyi (=solar) temperature ($T_{\rm eff}$ = 5800 K), and one-quarter solar surface gravity (log g = 1.84 m s^{-2}), close to the best estimates for β Hyi discussed in § 2. The simulations were made with a 32 × 32 × 32 spatial grid: 32 × 32 horizontal Fourier components over a stellar surface area of ≃12,000 km square, and with 32 knot points defining cubic splines for the vertical dependence of different parameters. The simulations were run for approximately 2 hr of stellar time, with a time step of 2 s. For a more detailed discussion of the stellar granulation modeling see Nordlund & Dravins (1990), and Dravins & Nordlund (1990a, b).

5.2.1. *Surface Structure of Temperature and Velocity*

As an example of the computed photospheric structure, Figure 3 shows a "snapshot" of the β Hyi model at a representative time, i.e., at an instant when its properties are roughly similar to the average for the full simulation. Temperature, pressure and velocities are shown at a fixed geometrical level near the stellar "surface." The hot granules are sharply delineated and correlate well with rising velocities. The horizontal velocity field shows where gases are transported from the upflows and into the downflow regions. The occasional lack of a detailed correlation with the superposed "granular" contours is due to the time history of the different features: old and decaying granules may already begin to be swept away by horizontal flows originating elsewhere.

Comparing to a corresponding solar model (with greater surface acceleration of gravity), the main difference to the β Hyi model is a corresponding change of geometric scales. For a given flow topology (in terms of the shape of the velocity field), a change in the density scale height implies that the horizontal scales must change with the same factor to still satisfy mass conservation. Additional effects come about because, with lower densities, the velocity amplitudes and/or the temperature contrast must be larger, to carry the same amount of convective energy flux (as required by the same effective temperature). We estimate that the velocity amplitudes are larger by about a factor ≃1.5 or 2 in the surface layers of the β Hyi model, relative to an equivalent solar one. Also, the temperature amplitudes increase with decreasing gravity. Apart from these changes of scales and amplitudes, the structure and topology of the granular gas flows are quite similar.

5.2.2. *Time Evolution of Granular Structure*

The simulations show the time evolution of the three-dimensional photospheric structures, in particular the hotter and generally rising granules. Their normal evolution typically involves a gradual increase in size until they disintegrate due to various causes.

Relatively undisturbed granules often grow to larger sizes, until they "collapse under their own weight." An upflow of hot gases at a few km s^{-1} from beneath the photosphere is required in order to carry the stellar convective heat flux outward. Upon reaching optically thin layers, these gases cool off and eventually turn around to descend in the cooler intergranular areas. The horizontal acceleration of the gases toward the sinking areas is accomplished by local overpressures that develop over granules (and also over intergranular lanes, in order to decelerate the incoming horizontal flow there). These mechanisms cause the pressure patterns (Fig. 3) to be more complicated than the temperature ones. The larger the granule, the larger the overpressure required to accelerate away the material over the greater horizontal distances. Ultimately, the overpressure on the surface becomes so great that it impedes the arrival of additional hot gases from below. Having been cut off from its energy supply, the granular center begins to cool off, a dark center develops, and the now ring-shaped granule disintegrates, a process apparently similar to solar "exploding granules." This mechanism limits the characteristic scale of granules on different stars: the granules cannot grow any larger because the required overpressure would block further convective energy supplies from beneath, thus strangling the granule through a lack of input heat. The characteristic scales in the β Hyi model are considerably larger than solar ones: $\lesssim 10^4$ km (reflecting the increased scale heights for density and pressure).

5.3. *Effects on Magnetic Fields*

The horizontal pressure differences that develop in response to the dynamical evolution of granulation also constrain the flux density to which photospheric magnetic fields are compressed. Detailed studies of the interaction between magnetic fields and granulation have previously been made for solar conditions (e.g., Nordlund 1986). Such simulations (as well as a general discussion of the situation) show that magnetic fields are rapidly emptied from the interiors of granules and are carried by the gas flows to the intergranular lanes, forming magnetic flux concentrations. These then remain in quasi-static equilibrium with their nonstationary granulation surroundings, and through the granular evolution they are constantly distorted and displaced (cf. also Spruit, Nordlund, & Title 1990).

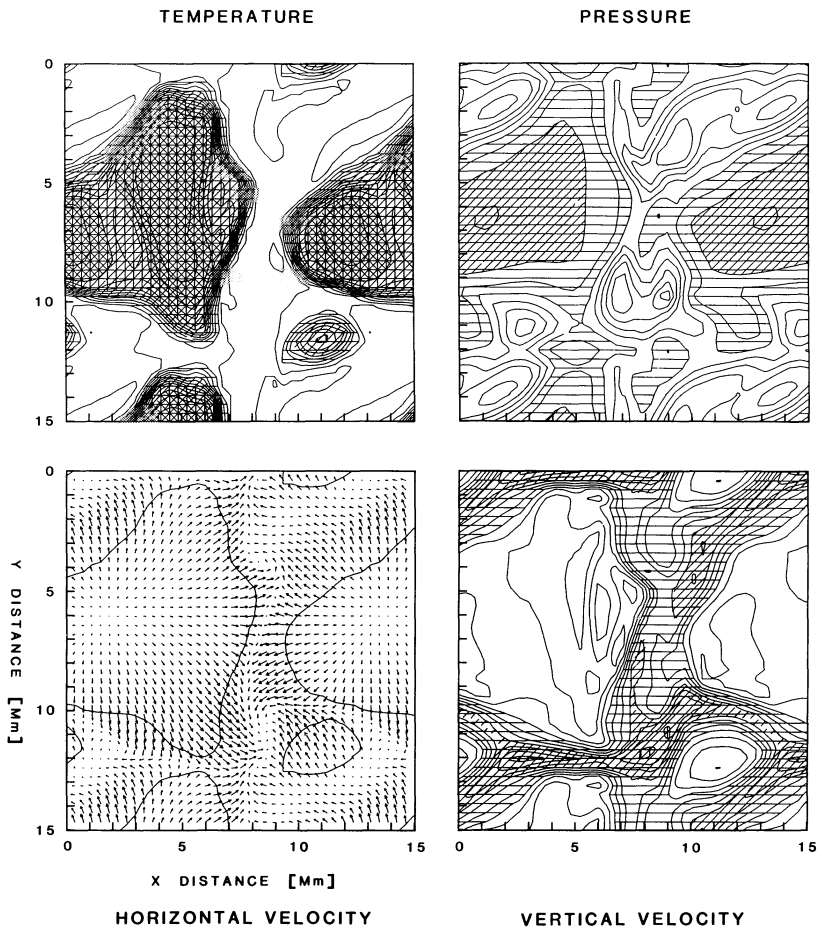

FIG. 3.—Overall appearance of the simulated stellar "surface" on β Hyi at a representative time. Temperature is shaded above $T_{\rm eff}$ = 5800 K, with contours in steps of 500 K. Pressure contours are every 0.05 dex, with shading above $10^{3.7}$ Pa. Downward velocities are shaded with contours every 1.0 km s^{-1}. Horizontal velocity vectors correspond to 60 s of motion, and superposed curves for $T_{\rm eff}$ = 5800 K delineate granule positions. Noteworthy in a comparison with the Sun are larger granules ($\lesssim$10,000 km), lower gas pressure, and more vigorous horizontal motions in higher layers.

Although the present simulations do not include magnetic fields, it is possible to make estimates of the effects on the small-scale magnetic fields on β Hyi, as compared to the situation on the Sun. The amount of photospheric flux concentration is largely set by the horizontal pressure differences that build up as a response to significant evacuation of the interior of magnetic flux tubes. On the Sun, these pressure differences permit magnetic fields of $\simeq$150 mT (1500 G) to be balanced. On β Hyi, the gas pressure at an optically equivalent "surface" layer is smaller by a factor of perhaps 2, and the corresponding pressure differences are also smaller, permitting only somewhat weaker fields to be supported. However, due to the interplay of several different factors, more precise statements will require detailed magnetohydrodynamic simulations.

5.4. *The Optical Appearance of Granulation*

The output from the model simulations has been used as a set of spatially and temporally variable model atmospheres, from which stellar surface images and spectral line profiles were computed. The numerical simulations provide three-dimensional parameter arrays, defining the photosphere at each moment in time. These data were used as input for radiative transfer calculations to compute the emerging continuum and line radiation for different spatial points, angles, wavelengths, and spectral line parameters. In Figure 4, synthetic continuum images are shown for the surface of the β Hyi model, at the same representative instant of time as in Figure 3. As expected, the geometrical shapes of granules at stellar disk center closely correspond to the temperature features. However, the intensity contrast is much lower than could have been naively expected from the temperature fluctuations at a constant geometrical depth: the opacities of overlying layers hide the larger temperature contrasts beneath.

Thus, the white-light appearance of the future Sun will not be drastically different from today, although the granules will become larger (by a factor of perhaps 5), display a somewhat greater optical contrast, and only a smaller number of them will fit on the stellar surface (perhaps only one-third of the 1–2 million currently present on the Sun). They will feature more rapid gas motions (by factors 1.5 or 2), with the gas pressure at an optically equivalent "surface" layer smaller by a factor of about 2, and the correspondingly lesser horizontal pressure differences will permit only somewhat weaker magnetic fields to be supported.

5.5. *Synthesis of Photospheric Line Profiles*

The simulation data were in particular used as input to compute photospheric line profiles. The radiative transfer was

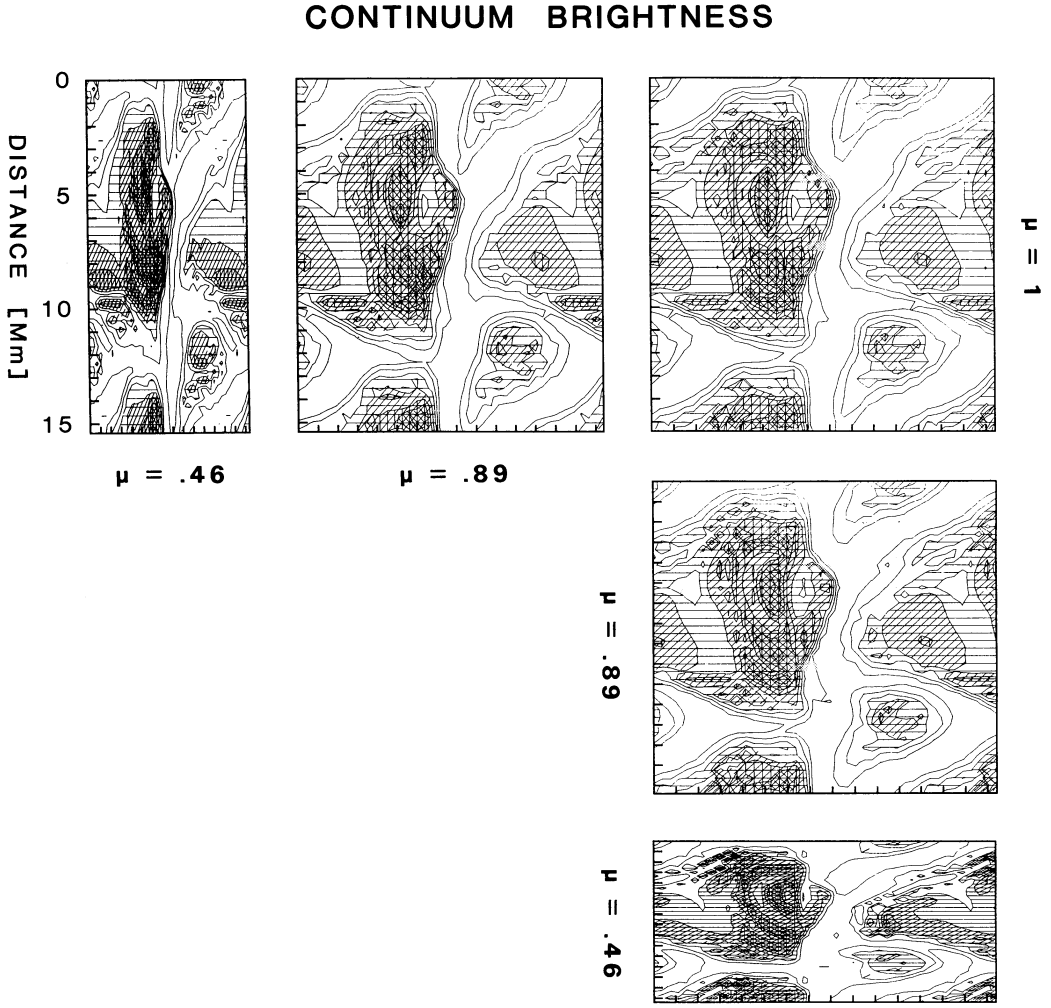

FIG. 4.—Synthetic white-light images (520 nm) of granulation in the hydrodynamic model of β Hyi. Images are shown for one region seen at stellar disk center ($\mu = 1$), and the same region seen toward the limb ($\cos\theta = \mu = 0.89$ and 0.46). Two different azimuth angles correspond to viewing the disk center image from the left or from below at successively more inclined angles. Areas brighter than average are shaded and contours are at every 20% of the average in each image.

solved for the inhomogeneous atmospheric structure along different rays throughout the simulation volume, for wavelengths every 1 km s^{-1} within ± 10 km s^{-1} of the rest wavelength. For each spectral line, and each geometric angle, such computations were made for all $32 \times 32 = 1024$ horizontal spatial elements at each step in time, and for some 100 time steps. By a suitable summation of spatially averaged data for different center-to-limb positions, disk-integrated line profiles are obtained as averages over the simulation sequence, permitting a direct comparison to observations. Most computations were made assuming local thermodynamic equilibrium. For a further discussion, see Dravins & Nordlund (1990a).

5.6. *Comparison to Observations*

5.6.1. *Observed Line Profiles*

The highest resolution data available on photospheric line profiles in β Hyi were obtained with the double-pass scanner of the coudé echelle spectrometer at the European Southern Observatory. In this observing mode, the light passes an intermediate slit inside the spectrometer to effectively remove scattered light, and then makes a second pass through the spectrometer. A very high spectral resolution ($\lambda/\Delta\lambda \simeq 200{,}000$) is obtained with a well-defined and very clean instrumental profile (Fig. 5), but at a high cost in photon efficiency. For these observations, the spectrometer was fed by the 3.6 m telescope through a 40 m long optical fiber. Besides for the required light collecting area, an additional reason for not using the ordinary 1.5 m coudé auxiliary telescope was that the nearby dome of the 3.6 m telescope blocks its view of the south celestial pole, and permits only rather marginal observations of far southern stars such as β Hyi ($\delta = -77°$). Even so, the limited brightness of β Hyi permitted only a few line profiles to be measured at this high resolution. For precise comparisons with the spectrum of the Sun seen as a star, sunlight was brought into the spectrometer through an optical fiber whose end (without optics) was pointed at the Sun. A representative observation is shown in Figure 5, while more details about the instrumentation and the observing methods are in Dravins (1987).

5.6.2. *Synthetic Spectral Lines*

The synthetic profiles for disk-integrated starlight were convoluted with profiles corresponding to the measured instru-

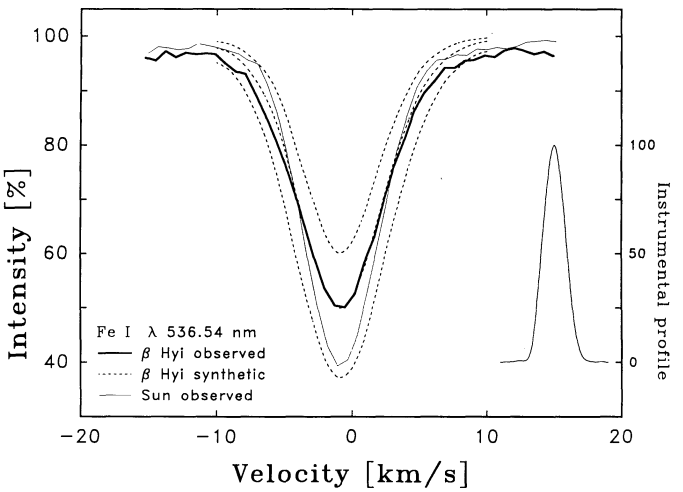

FIG. 5.—A representative photospheric Fe I line in β Hyi (*bold*), compared with synthetic profiles for differently strong lines computed from the hydrodynamic model (*dotted*), and the same line for the Sun seen as a star (*thin*). Photospheric lines are broader and shallower in β Hyi, as compared to the Sun. The increased width is largely due to a more vigorous granular convection, and the smaller depth partly to the smaller metallicity, while the rotational broadening is comparable.

mental ones, but slightly broadened to include effects of plausible amplitudes of stellar surface oscillations. For each value of the stellar rotational velocity, this produces a synthetic model grid of line profiles for differently strong spectral lines. Observed line profiles were then compared against these grids, and "best-fit" values of the projected stellar rotational velocity, $v \sin i$, deduced.

Observed and synthetic profiles for one representative photospheric Fe I absorption line are compared in Figure 5, which also shows the same line in integrated sunlight observed with the same instrument. This Fe I 536.54 nm line ($\chi = 3.57$ eV) is broader and shallower in β Hyi, as compared to the Sun. Three synthetic profiles for integrated starlight (520 nm, $\chi = 3$ eV) from the hydrodynamic simulation are shown. These differ only in their oscillator strengths, and the middle of the three is a fit to the observed line core, bracketed in Figure 5 by both a weaker and a stronger one. Besides simulated instrumental broadening, these have been rotationally broadened for $v \sin i = 2$ km s^{-1}. The wavelength scale (in velocity units) is *absolute* for the synthetic lines, i.e., "0" means a wavelength in integrated starlight equal to the laboratory one. The convective blueshift ($\simeq 800$ m s^{-1}) results from the velocity-brightness correlation in the photospheric granulation patterns. The observed line is on a *relative* wavelength scale only but has been plotted to match the synthetic ones. The inset at right shows the instrumental profile measured with a He-Ne laser in the ESO double-pass scanner used, operated at a nominal spectral resolution $\lambda/\Delta\lambda \simeq 200{,}000$. The data were sampled with a step size of 1.3 pm (13 mÅ), and for each step, some 95,000 or 220,000 photon counts were accumulated in the continuum for β Hyi and sunlight, respectively.

Such fits for different Fe I lines gives $v \sin i \simeq 2 \pm 1$ km s^{-1} (Dravins & Nordlund 1990b). This value is consistent with β Hyi having had a main-sequence rotation rate similar to that of the present Sun.

As seen in Figure 5, the synthetic line *cores* agree well with observed ones, but there is inadequate absorption in the synthetic line *wings* outside about ± 5 km s^{-1}. Corresponding fits of synthetic solar profiles give almost perfect agreement with observations, also in the line wings. It is believed that this missing broadening in the β Hyi line wings is an artifact of the hydrodynamically anelastic model, which does not handle sound waves. The granulation in β Hyi is more vigorous than that in the Sun, and horizontal velocities reach quite large amplitudes in the upper photosphere. Due to the inherent limitations in the present model, these velocities had to be numerically constrained before becoming supersonic. The line wing absorption is largely due to rapidly moving horizontal features, observed away from stellar disk center, with only a modest contribution from occasional rapid vertical motions. A removal of the anelastic approximation in the models will allow sound and shock waves to develop and include the missing line broadening from horizontal features moving at (super)sonic speed, Such computations have been carried out for the Sun (Stein, Nordlund, & Kuhn 1989), and the application of such more realistic models would seem a priority item for future work.

6. CONCLUSIONS

β Hydri was selected as a proxy for the future Sun, and its properties carefully scrutinized. Combining evolutionary calculations with best estimates for its luminosity, we find its age $\simeq 9.5$ Gyr, a value which fits well with current estimates of the age of the Galactic disk. We conclude that, by all appearances, β Hyi seems to be a normal and typical star of the old disk population. Examining its evolutionary history, it seems to have been as close to the Sun in physical properties as is reasonably possible for any star born in the early life of the Galaxy. Therefore, as a case study, it should represent one of the best possible illustrations of the likely distant future of the Sun.

Although the lithium abundance in β Hyi is much higher than solar, and on first sight could have suggested a stellar youth, it in no way appears unusual among old subgiants. A plausible scenario for the lithium enhancement involves diffusion in the radiatively stable layers beneath the surface convection zone during the latter main-sequence lifetime. This is followed by a dredge-up of lithium to the surface as the convection zone begins to reach deeper during the early subgiant stage. With its otherwise well-studied properties, β Hyi can become a suitable object for the testing of detailed theories of lithium depletion, and perhaps even of the evolution of rotation inside solar-type stars.

The photospheric fine structure of the future Sun was studied through simulations in numerical hydrodynamics. The white-light appearance of the stellar surface will not be drastically different from today, although the scale of the photospheric granulation will become larger (by a factor of perhaps 5), the granules will have a somewhat greater white-light contrast, and only a smaller number of them will fit on the star (possibly only one-third of the 1–2 million currently present on the Sun). They will feature more rapid gas motions (by factors of 1.5 or 2), with the gas pressure at an optically equivalent "surface" layer smaller by a factor of about 2, and the correspondingly smaller horizontal pressure differences will permit only somewhat weaker small-scale magnetic fields to be supported.

Comparing observed Fe I photospheric absorption line profiles with those synthesized from hydrodynamic models yields a value for the stellar rotation $v \sin i \simeq 2 \pm 1$ km s^{-1}, consistent with β Hyi having had a main-sequence rotation rate similar to that of the present Sun. The rotational velocity at the

solar equator is 1.8 km s^{-1}. Since the radius of β Hyi is approximately $1\frac{1}{2}$ times solar, a given velocity implies a correspondingly longer rotational period. Assuming the rotational axis in the plane of the sky, 2 km s^{-1} implies a period of about 45 days.

With this enhanced understanding of the general stellar properties, the deeper atmospheric layers, and the photosphere, we now proceed to a detailed examination of the chromospheric activity in β Hyi, and its time variability. That is the topic of Paper II in this series.

The Swedish part of this project was supported by the Swedish Natural Science Research Council. We thank G. Lund at ESO for advice on operating the fiber optics link from the 3.6 m telescope to the coudé echelle spectrometer. The discussion of stellar structure, and lithium evolution benefited from discussions with C. Deliyannis (formerly at Yale, now in Honolulu). M. Wenger (Strasbourg) gave advice on how to search the SIMBAD data base, and J. L. Linsky (Boulder) contributed many helpful comments.

REFERENCES

Abt, H. A., & Biggs, E. S. 1972, Bibliography of Stellar Radial Velocities (New York: np)
Andersen, J., Clausen, J. V., Gustafsson, B., Nordström, B., & VandenBerg, D. A. 1988, A&A, 196, 128
Andersen, J., Gustafsson, B., & Lambert, D. L. 1984, A&A, 136, 65
Beckers, J. M., Bridges, C. A., & Gilliam, L. B. 1976, A High Resolution Spectral Atlas of the Solar Irradiance from 380 to 700 Nanometers (Sunspot, NM: Sacramento Peak Observatory)
Beckman, J. E., Crivellari, L., & Selvelli, P. L. 1982, A&AS, 47, 295
Cayrel de Strobel, G. 1981, Bull. Inform. CDS, 20, 28
Crawford, D. L. 1975, AJ, 80, 955
Deliyannis, C. P., Demarque, P., & Kawaler, S. D. 1990, ApJS, 73, 21
Dravins, D. 1987, A&A, 172, 211
Dravins, D., Linde, P., Ayres, T. R., Linsky, J. L., Monsignori-Fossi, B., Simon, T., & Wallinder, F. 1993b, ApJ, 403, 412 (Paper III)
Dravins, D., Linde, P., Fredga, K., & Gahm, G. F. 1993a, ApJ, 403, 396 (Paper II)
Dravins, D., & Nordlund, Å. 1990a, A&A, 228, 184
———. 1990b, A&A, 228, 203
Duncan, D. K. 1981, ApJ, 248, 651
Edmonds, P. D., & Cram, L. E. 1989, Proc. Astron. Soc. Australia, 8, 154
———. 1990, BAAS, 22, 817
Eggen, O. J. 1958, MNRAS, 118, 154
———. 1971, PASP, 83, 251
Evans, D. S., Menzies, A., & Stoy, R. H. 1957, MNRAS, 117, 534
Feast, M. W. 1966, MNRAS, 134, 321
———. 1970, MNRAS, 148, 489
Frandsen, S. 1987, A&A, 181, 289
Gehren, T. 1981, A&A, 100, 97
Gilliland, R. L. 1985, ApJ, 299, 286
Gratton, R. G., & Ortolani, S. 1986, A&A, 169, 201
Guenther, D. B. 1991, ApJ, 375, 352
Hearnshaw, J. B. 1972, MmRAS, 77, 55
———. 1973, in IAU Coll. 17, ed. G. Cayrel de Strobel & A. M. Delplace, L'Âge des Étoiles, p. XLI-1
Hobbs, L. M., & Pilachowski, C. 1988, ApJ, 334, 734
Hoffleit, D., & Jaschek, C. 1982, The Bright Star Catalogue (4th ed.; New Haven: Yale University Obs.)
Jenkins L. F. 1952, General Catalogue of Trigonometric Stellar Parallaxes (New Haven: Yale University Obs.)
Krishna Swamy, K. S. 1966, ApJ, 145, 174
Kukarkin, B. V., Parenago, P. P., Efremov, J. I., & Holopov, P. N. 1951, Katalog zvezd zapodozrennyh v peremennosti (Catalogue of stars of suspected variability), (Moscow: Akademia Nauk)
Kukarkin, B. V., et al. 1982, Novyj katalog zvezd zapodozrennyh v peremennosti bleska (New catalogue of suspected variable stars), (Moscow: Nauka)
Maurice, E., Spite, F., & Spite, M. 1984, A&A, 132, 278
Michaud, G., & Charbonneau, P. 1991, Space Sci. Rev., 57, 1
Nordlund, Å. 1982, A&A, 107, 1
———. 1985, Sol. Phys., 100, 209
———. 1986, in Small Scale Magnetic Flux Concentrations in the Solar Photosphere, ed. W. Deinzer, M. Knölker, & H. H. Voigt (Göttingen: Van den Hoeck & Ruprecht), 83
Nordlund, Å., & Dravins, D. 1990, A&A, 228, 155
Pallavicini, R., Cerruti-Sola, M., & Duncan, D. K. 1987, A&A, 174, 116
Perrin, M. N., Hejlesen, P. M., Cayrel de Strobel, G., & Cayrel, R. 1977, A&A, 54, 779
Pinsonneault, M. H., Kawaler, S. D., Sofia, S., & Demarque, P. 1989, ApJ, 338, 424
Proust, D., & Foy, R. 1988, Ap&SS, 145, 61
Randich, S., & Pallavicini, R. 1991, Mem. Soc. Astron. Ital., 62, 75
Rebolo, R., Crivellari, L., Castelli, F., Foing, B., & Beckman, J. E. 1986, A&A, 166, 195
Rebolo, R., Molaro, P., & Beckman, J. E. 1988, A&A, 192, 192
Rodgers, A. W., & Bell, R. A. 1963, Observatory, 83, 79
Ruciński, S. M., & VandenBerg, D. A. 1986, PASP, 98, 669
Simon, T. 1992, in The Seventh Cambridge Workshop on Cool Stars, Stellar Systems, and the Sun, ed. M. S. Giampapa, & J. A. Bookbinder (ASPC 26), 3
Soderblom, D. R., Duncan, D. K., & Johnson, D. R. H. 1991, ApJ, 375, 722
Spruit, H. C., Nordlund, Å, & Title, A. M. 1990, ARA&A, 28, 263
Stein, R. F., Nordlund, Å., & Kuhn, J. R. 1989, in Solar and Stellar Granulation, ed. R. J. Rutten & G. Severino (Dordrecht: Kluwer), 381
Stobie, R. S. 1971, M.N.A.S.So. Africa, 30, 31
VandenBerg, D. A. 1983, ApJS, 51, 29
VandenBerg, D. A., & Bell, R. A. 1985, ApJS, 58, 561
VandenBerg, D. A., & Laskarides, P. G. 1987, ApJS, 64, 103
Zinner, E. 1929, Astronomische Abhandlungen 8, Nr. 1, A1